Moniliformis cryptosaudi *n. sp. (Acanthocephala: Moniliformidae) from the Long-eared Hedgehog* Hemiechinus auritus *(Gmelin) (Erinaceidae) in Iraq; A Case of Incipient Cryptic Speciation Related to* M. saudi *in Saudi Arabia*

Omar M. Amin, Richard A. Heckmann, Meysam Sharifdini & Nagham Yaseen Albayati

Acta Parasitologica

ISSN 1230-2821

Acta Parasit.
DOI 10.2478/s11686-018-00021-9

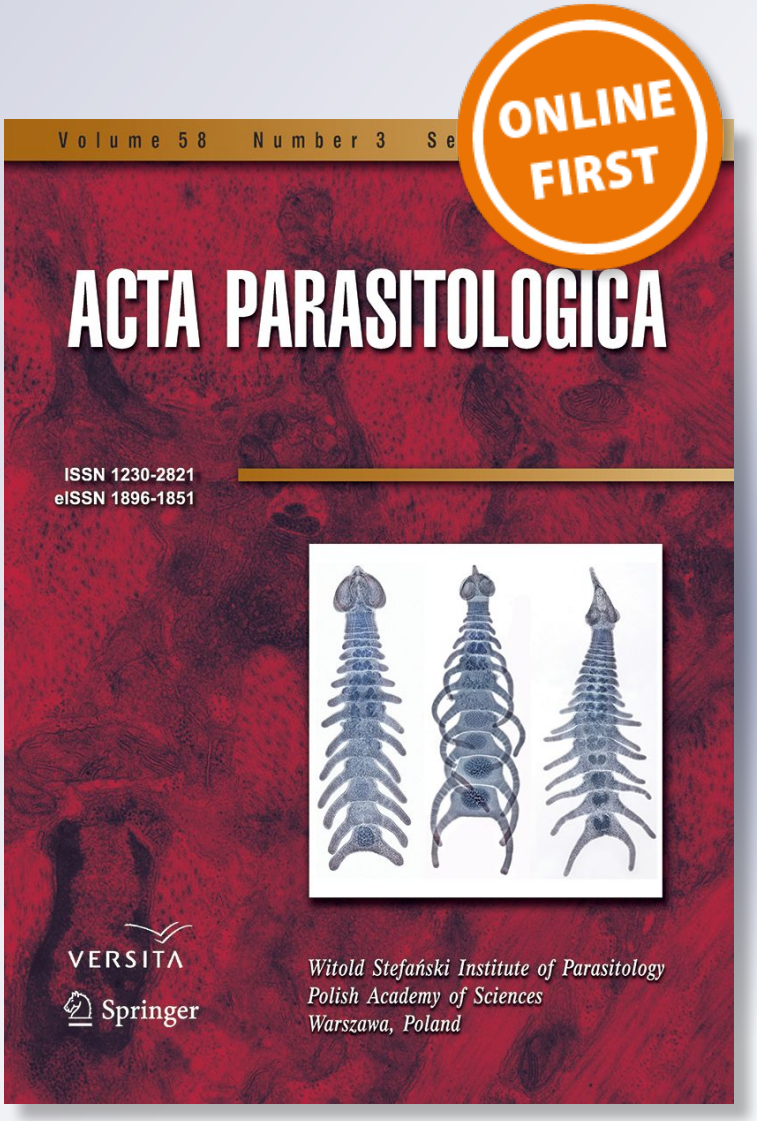

Springer

Acta Parasitologica
https://doi.org/10.2478/s11686-018-00021-9

ORIGINAL PAPER

Moniliformis cryptosaudi n. sp. (Acanthocephala: Moniliformidae) from the Long-eared Hedgehog *Hemiechinus auritus* (Gmelin) (Erinaceidae) in Iraq; A Case of Incipient Cryptic Speciation Related to *M. saudi* in Saudi Arabia

Omar M. Amin[1] · Richard A. Heckmann[2] · Meysam Sharifdini[3] · Nagham Yaseen Albayati[4]

Received: 23 July 2018 / Accepted: 13 December 2018

Abstract
Moniliformis cryptosaudi n. sp. (Moniliformidae) is an acanthocephalan described from the long-eared hedgehog *Hemiechinus auritus* (Gmelin) (Erinaceidae) in Iraq as an incipient cryptic species of *Moniliformis saudi* Amin, Heckmann, Mohammed, Evans, 2016 described from the desert hedgehog *Paraechinus aethiopicus* (Ehrenberg) (Erinaceidae) in Saudi Arabia. Microscopical studies demonstrate that the two species are morphologically indistinguishable with practically identical measurements and counts but differed significantly in their energy dispersive X-ray analysis (EDXA) of metal composition of hooks. Hooks of specimens of the new species appeared to be of collagen material with very low levels of phosphorus and calcium unlike those of *M. saudi* and *Moniliformis kalahariensis* Meyer, 1931 that had high levels of calcium and phosphorus. Using 18S rDNA and *cox1* genes, *M. Saudi* and *M. kalahariensis* were shown to be molecularly distinct but the molecular profiles of *M. saudi* and *M. cryptosaudi* were more similar. The molecular profile of *M. kalahariensis* collected from the South African hedgehog *Atelerix frontalis* Smith (Erinaceidae) in South Africa is reported for the first time and is studied only for comparative purposes. *Moniliformis saudi* and *M. kalahariensis* had comparable EDXA metal analysis that was distinct from that of *M. cryptosaudi*.

Keywords Acanthocephala · *Moniliformis cryptosaudi* · *M. saudi* · *M. kalahariensis* · Molecular profiles · Metal analysis of hooks

Introduction

The literature on cryptic speciation in the Acanthocephala has been slowly gaining exposure over the last few years as morphologically similar but genetically distinct species are becoming recognized and described. Steinauer et al. [17] explored cryptic speciation and patterns of phenotypic variation in the highly variable species *Leptorhynchoides thecatus* (Linton, 1891) Kostylew, 1924 in North America. Martinez-Aquino et al. [12] detected a complex of cryptic species within 12 populations of *Neoechinorhynchus golvani* Salgado-Maldonado, 1978 (Neoechinorhynchidae) parasitizing freshwater and brackish water fishes in Mexico and one population in Costa Rica. Pinacho-Pinacho et al. [16] subsequently qualified the "hyper-diverse" genus *Neoechinorhynchus* Stiles et Hassall, 1905 using tree-based and non-tree-based species delimitation methods revealing 10 cryptic species of *Neoechinorhynchus* in Middle American freshwater fishes. Zittel et al. [18] characterized 3 cryptic species of *Polymorphus minutus* (Goeze, 1782) Lühe, 1911 (Polymorphidae) and examined their utilization of indigenous and non-indigenous intermediate hosts from 27 different sites in Germany and France. Nadler and Pérez-Ponce de León [13] reviewed the theoretical and methodological

✉ Omar M. Amin
omaramin@aol.com

[1] Institute of Parasitic Diseases, 11445 E. Via Linda 2-419, Scottsdale, AZ 85259, USA

[2] Department of Biology, Brigham Young University, 1114 MLBM, Provo, UT 84602, USA

[3] Department of Medical Parasitology and Mycology, School of Medicine, Guilan University of Medical Sciences, Rasht, Iran

[4] Biology Department, College of Education for Pure Sciences, Diyala University, Diyala, Iraq

Published online: 21 January 2019

considerations important for finding and delimiting cryptic species of parasites (species that are difficult to recognize using traditional systematic methods) and examined the applications of molecular data in empirical investigations of cryptic species. Goulding and Cohen [6] demonstrated the lack of cryptic diversity in *Profilicollis altmani* infecting three species of *Emerita* crabs of the Pacific, Atlantic and Gulf coasts of the USA, and the Pacific coast of Panama and Chile. We, Amin et al. [2], have demonstrated cryptic diversity in *Tenuisentis niloticus* (Meyer, 1932) (Tenuisentidae) from *Heterotis niloticus* (Cuvier) in Burkina Faso. Pérez-Ponce de León and Nadler [15] noted the lack of methodological and theoretical uniformity in the finding and delimiting cryptic species, drew attention to the need for standardizing these approaches, and recommended that "parasitologists describe (and formally name) cryptic species following standard taxonomic practice" which is the subject matter of this paper.

We have been recently presented with a case in a point of the incipient cryptic acanthocephalan *Moniliformis cryptosaudi* n. sp. (Moniliformidae) being described from the long-eared hedgehog *Hemiechinus auritus* (Gmelin) (Erinaceidae) in Iraq and of *Moniliformis saudi* Amin, Heckmann, Mohammed, Evans, 2016 described from the desert hedgehog *Paraechinus aethiopicus* (Ehrenberg) (Erinaceidae) in Saudi Arabia. The two species are morphologically indistinguishable using regular microscopy but differed significantly in their energy dispersive X-ray analysis (EDXA) of metal composition of hooks. Hooks of specimens of *M. cryptosaudi* appeared to be of collagen material with negligible levels of phosphorus and calcium compared to those of *M. saudi* and *M. kalahariensis*. The latter species was collected from the South African hedgehog *Atelerix frontalis* Smith (Erinaceidae) in South Africa and was studied for comparison. We have studied the morphological features, metal analysis and molecular profile of these 3 taxa to explore their inter-relationship especially regarding the potential cryptic status of the Iraqi material.

Materials and Methods

Collections

One hundred and seventeen specimens of the acanthocephalan *Moniliformis cryptosaudi* n. sp. were collected by one of us (NYA) from 20 of 38 individuals of the long-eared hedgehog *Hemiechinus auritus* (Gmelin) (Erinaceidae) in various agrarian townships around Baquba, Diyala Governerate (33°53′N 45°4′E), east-central Iraq between October 2016 and April 2017 (Table 1). A few additional worms were collected subsequently to ship to one of us (MS) Iran for molecular studies. Specimens of *Moniliformis kalahariensis* Meyer, 1931 collected from the South African hedgehog *Atelerix frontalis* Smith (Erinaceidae) in South Africa by Ali Halajian, Limpopo University, were sent to OMA for

Table 1 Collections of specimens of *Moniliformis cryptosaudi* from 20 of 38 examined *Hemiechinus auritus* in Baquba, Iraq

Host no.	Date of capture	Date of dissection	Collection site	Host sex	No. of parasites
1	10-23-2016	10-24-2016	Buhriz in Baquba	Female	1
2	10-26-2016	10-27-2016	Buhriz in Baquba	Female	2
3	10-26-2016	10-27-2016	Buhriz in Baquba	Female	9
4	10-28-2016	10-29-2016	Kinaan in Baquba	Male	24
5	11-1-2016	11-2-2016	Kinaan in Baquba	Female	1
6	11-1-2016	11-2-2016	Kinaan in Baquba	Female	4
7	11-2-2016	11-3-2016	Hedaid in Baquba	Female	2
8	11-8-2016	11-10-2016	Khan Bani Saad in Baquba	Female	4
9	11-19-2016	11-10-2016	Kinaan in Baquba	Female	5
10	11-23-2016	11-14-2016	Kinaan in Baquba	Male	1
11	11-23-2016	11-25-2016	Khan Bani Saad in Baquba	Female	4
12	11-24-2016	11-26-2016	Khan Bani Saad in Baquba	Female	24
13	12-5-2016	12-6-2016	Hedaid in Baquba	Male	5
14	12-6-2016	12-8-2016	Hedaid in Baquba	Female	8
15	12-26-2016	12-27-2016	Kinaan in Baquba	Male	4
16	3-26-2017	3-27-2017	Hedaid in Baquba	Male	6
17	3-27-2016	3-28-2017	Kinaan in Baquba	Female	7
18	4-8-2017	4-9-2017	Kinaan in Baquba	Male	1
19	4-1-2017	4-2-2017	Khan Bani Saad in Baquba	Female	3
20	4-20-2017	4-21-2017	Khan Bani Saad in Baquba	Female	2

examination and to MS in Iran for comparative molecular studies.

Freshly collected specimens were extended in water until proboscides everted then fixed in 70% ethanol for transport to our Arizona, USA laboratory for processing and further studies by OMA and RAH.

Materials Examined

Of 117 specimens of *M. cryptosaudi* collected from *H. auritus* in Iraq (Table 1), 103 were studied microscopically including nine males and 13 females that were measured, six were processed for SEM studies, and 8 for molecular study. Eleven and 17 male and female specimens of *M. saudi* were similarly studied (Table 2) [2]. Microscopical pictures, SEM images, X-ray scans, complete measurements, and descriptive accounts of both sexes of the new species are provided herein for the first comprehensive description of the new species. See Amin et al. [3] for corresponding information of *M. saudi*. Only line drawings were not made of *M. cryptosaudi* as its morphology is practically identical to that of *M. saudi*. Specimens of *M. kalahariensis* from South Africa were also used for molecular analysis. SEM and EDXA images of all three

Table 2 Morphometrics of *Moniliformis saudi* from *Paraechinus aethiopicus* in Saudi Arabia and *M. cryptosaudi* from *Hemiechinus auritus* in Iraq

Structures	Males		Females	
	Saudi Arabia ($N=11$)	Iraq ($N=9$)	Saudi Arabia ($N=17$)	Iraq ($N=13$)
Trunk (mm)	24.00–50.00 (35) × 0.67–1.15 (0.94)	20.50–48.75 (30.75) × 0.72–1.05 (0.86)	18.00–117.50 (55.60) × 0.60–1.82 (1.18)	28.75–121.25 (53.59) × 0.65–2.25 (1.23)
Giant nuclei (L, D, V)*	11–43 (19), 2–12 (9), 4–17 (10)	7–31 (15), 4–10 (7) 6–9 (8)	11–43 (19), 2–12 (9) 4–17 (10)	14–28 (21), 3–6 (5) 5–15 (9)
Proboscis	315–520 (396) × 130–177 (150)	343–416 (364) × 135–188 (165)	354–468 (406) × 130–208 (170)	300–416 (370) × 162–291 (207)
Hook rows × H/row	13–14 × 8	13–14 (13.5) × 7–8 (7.8)	13–14 × 7–8	13–14 (13.4) × 7–8 (7.4)
Hook length from anterior	25–27 (26), 25–26 (26)	16–25 (22), 17–25 (22)	25–31 (28), 22–28 (25)	25–35 (29), 23–32 (29)
	25–27 (26), 22–25 (24)	17–27 (22), 20–25 (21)	22–25 (24), 20–25 (22)	22–30 (26), 20–30 (25)
	20–25 (23), 20–21 (21)	20–25 (21), 17–20 (19)	17–25 (21), 15–23 (19)	20–27 (23), 18–27 (22)
	17–21 (19), 15–17 (16)	17–20 (18), 15–17 (16)	15–21 (17), 15–20 (17)	17–27 (21), 16–25 (18)
Receptacle	603–880 (732) × 190–300 (237)	551–936 (775) × 200–291 (236)	718–1250 (987) × 155–322 (271)	624–1092 (950) × 218–364 (267)
Long lemniscus (mm)	2.91–8.75 (4.68) × 0.08–0.17 (0.13)	4.26–7.28 (6.11) × 0.12–0.18 (0.15)	3.30–12.50 (7.78) × 0.11–0.22 (0.18)	4.15–8.12 (5.63) × 0.11–0.21 (0.14)
Short lemniscus (mm)	2.81–5.75 (13.94) × 0.07–0.14 (0.11)	3.74–5.72 (4.0) × 0.09–0.15 (0.12)	3.02–11.25 (7.16) × 0.10–0.17 (0.16)	2.18–7.25 (4.65) × 0.11–0.21 (0.14)
Lemniscal nuclei (L, S)**	7–10	6–8 (7) (L), 3–4 (3) (S)	7–10	6–9 (7) (L), 5–6 (6) (S)
Ant. testis (mm)	1.25–3.50 (2.19) × 0.27–0.82 (0.56)	1.65–3.67 (2.40) × 0.40–0.62 (0.50)		
Post. testis (mm)	1.12–3.50 (2.19) × 0.27–0.65 (0.47)	1.50–2.62 (2.40) × 0.37–0.62 (0.48)		
Cement glands	312–811 (563) × 270–468 (341)	322–780 (570) × 229–416 (311)		
Saefftigen's pouch	468–1400 (830) × 177–450 (290)	624–925 (797) × 270–425 (326)		
Reproductive syst. (mm)			1.25–1.56 (1.36) 2.4% of trunk	0.85–1.35 (1.12) 2.1% of trunk
Eggs			57–83 (67) × 31–42 (34)	50–104 (71) × 25–36 (28)

*Range and average number of lateral (L), dorsal (D), and ventral (V) sub cutaneous giant nuclei

**Range and average number of giant nuclei in anterior half of long (L) and short (S) lemnisci

species and specimens of each species in OMA collection were studied anew for comparative purposes.

Methods

Processing for Microscopical Studies

Worms were punctured with a fine needle and subsequently stained in Mayer's acid carmine, destained in 4% hydrochloric acid in 70% ethanol, dehydrated in ascending concentrations of ethanol (24 h each), and cleared in 100% xylene then in 50% Canada balsam and 50% xylene (24 h each). Whole worms were then mounted in Canada balsam. Measurements are in micrometers, unless otherwise noted; the range is followed by the mean values between parentheses. Width measurements represent maximum width. Trunk length does not include proboscis, neck, or bursa. Line drawings were created by a Ken-A-Vision micro-projector (Ward's Biological Supply Co., Rochester, NY) which uses cool quartz iodine 150 W illumination. Color-coded objectives, 10×, 20×, and 43× lenses, are used. Images of stained whole mounted specimens were projected vertically on 300 series Bristol draft paper (Starthmore, Westfield, Massachusetts), then

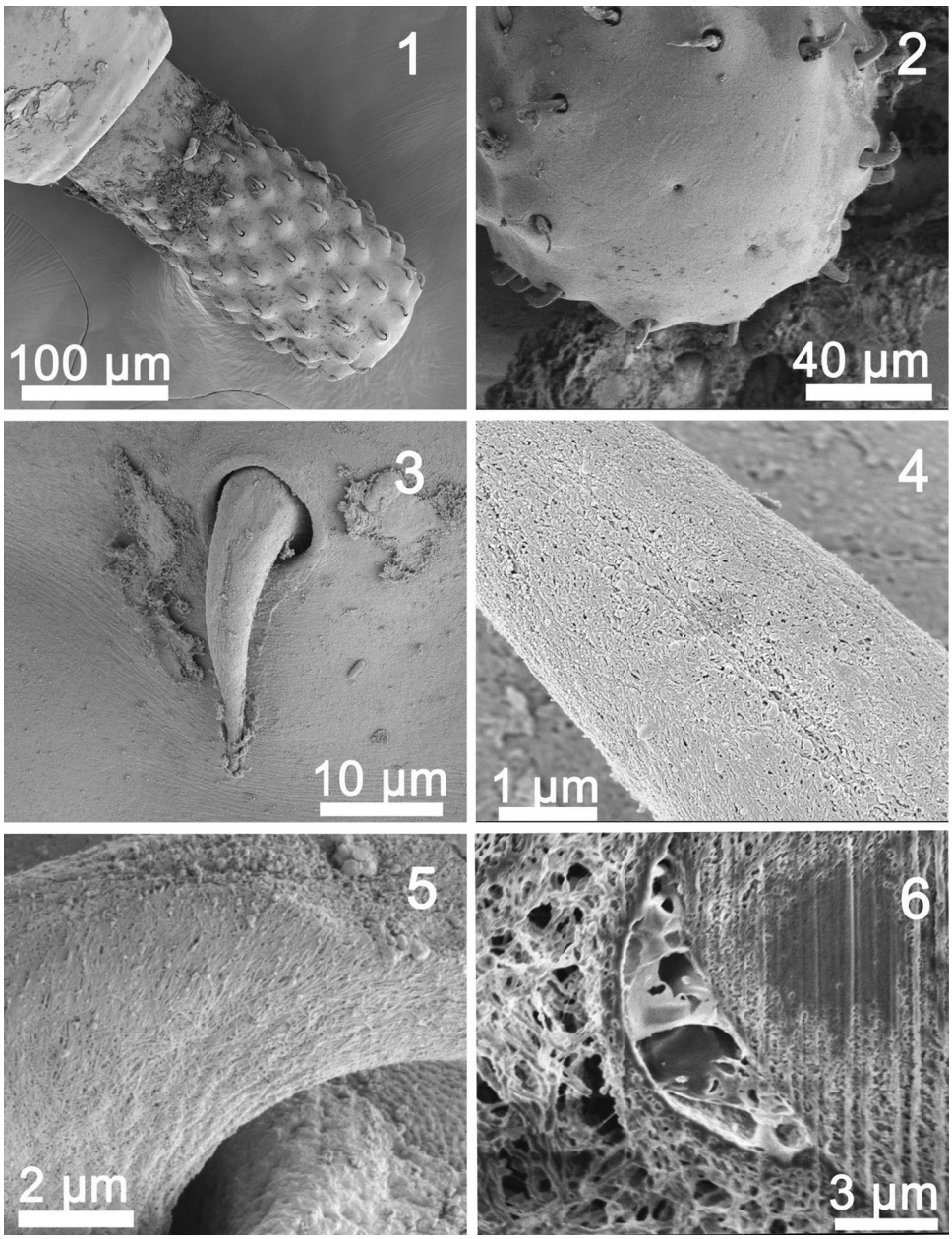

Figs. 1–6 SEM of proboscis and hooks of specimens of *Moniliformis cryptosaudi* n. sp. from the long-eared hedgehog *Hemiechinus auritus* (Gmelin) (Erinaceidae) in Iraq. **Fig. 1** The proboscis of a male paratype. **Fig. 2** An apical view of the proboscis in **Fig. 1** showing the two sensory pores also characteristic of specimens of *M. saudi*. **Figs. 3**, **4**. A posterior proboscis hook and a highly magnified view of an anterior hook showing the porous texture of its collagenous forming elements. **Figs. 5**, **6**. Perspectives of two gallium cut hook base sections showing their collagenous porous and spongy textures

traced and inked with India ink. Projected images were identical to the actual specimens being projected. The completed line drawings were subsequently scanned at 600 pixels on a USB and subsequently downloaded on a computer.

Type specimens were deposited in the University of Nebraska's State Museum's Harold W. Manter Laboratory (HWML) collection in Lincoln, Nebraska, USA.

Scanning Electron Microscopy (SEM)

Six specimens that had been fixed and stored in 70% ethanol were processed for SEM following standard methods [11]. These included critical point drying (CPD) in sample baskets and mounting on SEM sample mounts (stubs) using conductive double-sided carbon tape. Samples were coated with gold and palladium for 3 min using a Polaron #3500 sputter coater (Quorum (Q150 TES) www.quorumtech.com) establishing an approximate thickness of 20 nm. Samples were placed and observed in an FEI Helios Dual Beam Nanolab 600 (FEI, Hillsboro, Oregon) Scanning Electron Microscope with digital images obtained in the Nanolab software system (FEI, Hillsboro, Oregon) and then transferred to a USB for future reference. Samples were received under low vacuum conditions using 10 kV, spot size 2, 0.7 Torr using a GSE detector.

X-ray Microanalysis, Energy Dispersive X-ray Analysis (EDXA)

Standard methods were used for preparation similar to the SEM procedure. Specimens were examined and positioned with the above SEM instrument which was equipped with a Phoenix energy dispersive X-ray analyzer (FEI, Hillsboro, Oregon). X-ray spot analysis and live scan analysis were performed at 16 kV with a spot size of 5 and results were recorded on charts and stored with digital imaging software attached to a computer. The Texture and Elemental Analytical Microscopy (TEAM*) software system (FEI, Hillsboro, Oregon) was used. Data were stored in a USB for future analysis. The data included weight percent and atom percent of the detected elements following correction factors.

Ion Sectioning of Hooks

A dual-beam SEM with a gallium (Ga) ion source (GIS) is used for the liquid ion metal source (LIMS) part of the process. The hooks of the acanthocephalans were centered on the SEM stage and cross sectioned using a probe current between 0.2 and 2.1 nA according to the rate at which the area is cut. The time of cutting is based on the nature and sensitivity of the tissue. Following the initial cut, the sample also goes through a milling process to obtain a smooth surface. The cut was then analyzed with X-ray at the tip, middle, and base of hooks for chemical ions with an electron beam (tungsten) to obtain an X-ray spectrum. Results were stored with the attached imaging software, then transferred to a USB for future use. The intensity of the GIS was variable according to the nature of the material being cut.

Molecular Studies

The genomic DNA was extracted from 70% ethanol-preserved specimens using a commercial kit (High Pure PCR Template Preparation Kit; Roche, Mannheim, Germany) according to the manufacturer's recommended protocol. Forward primer (5′-AGATTAAGCCATGCATGCGTAAG-3′) and reverse primer (5′-TGATCCTTCTGCAGGTTCACC TAC-3′) were used for the amplification of a 1685 bp fragment of the nuclear 18S rDNA gene [14]. Also, a 664 bp fragment of the mitochondrial cytochrome oxidase subunit 1 gene (COX1) was amplified using the primers COI-F (5′-AGTTCTAATCATAARGATATYGG-3′) and COI-R (5′-TAAACTTCAGGGTGACCAAAAAATCA-3′) [5].

PCR reaction was performed in a 30-µl reaction mixture containing 15 µl of PCR mix including 1.25 U Taq DNA polymerase, 200 µM of dNTPs and 1.5 mM $MgCl_2$ (2 × Master Mix RED Ampliqon, Denmark), 10 pmol of each primer and 2 µl of DNA sample. The thermal PCR profiles for 18S rRNAgene included an initial denaturation step at 95 °C for 6 min followed by 35 cycles of denaturation at 95 °C for 30 s, annealing at 57 °C for 30 s and extension at 72 °C for 90 s, followed by a final extension step at 72 °C for 6 min. PCR conditions of cox1 gene amplification consisted of initial denaturation at 95 °C for 6 min, 35 cycles of 95 °C for 30 s, 55 °C for 30 s, and 72 °C for 1 min, followed by a final extension at 72 °C for 6 min. The amplified products

Table 3 Results of X-ray scans of gallium cuts of hooks of three species of *Moniliformes*

Hook Parts	*M. saudi*	*M. kalaharensis*	*M. cryptosaudi*
Hook tip			
P	12.15[a]	9.64	0.27
S	0.29	0.67	0.84
Ca	24.73	12.23	0.19
Hook middle			
P	7.58	15.91	0.44
S	0.11	0.09	0.22
Ca	19.03	31.15	0.42
Hook base			
P	14.21	15.80	1.01
S	0.21	0.13	0.74
Ca	34.45	38.15	0.99

[a]Cut % of P = phosphorus, S = sulfur, Ca = calcium

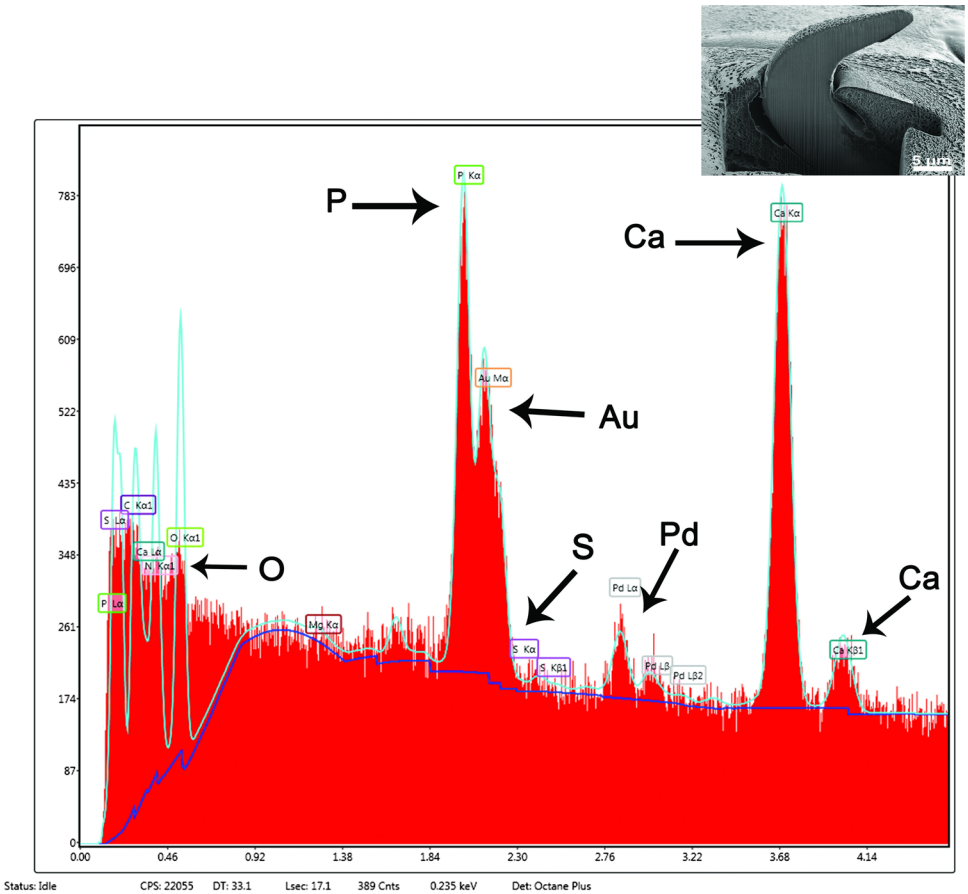

Element	Weight %	Atomic %	Error %	Net Int.	K Ratio
C K	8.93	14.97	11.13	147.79	0.0363
N K	27.58	39.66	12.58	190.02	0.0496
O K	23.14	29.13	11.7	305.59	0.0384
Mg K	0.07	0.06	77.17	4.94	0.0004
P K	7.58	4.93	6.79	573.22	0.0646
Au M	10.71	1.09	11.86	353.38	0.0923
S K	0.11	0.07	64.95	7.58	0.0009
Pd L	2.86	0.54	34.09	85.96	0.0211
Ca K	19.03	9.56	4.98	796.84	0.168

Fig. 7 X-ray elemental scan (XEDS) of the center of a *Moniliformis saudi* hook showing high levels of calcium and phosphorus; see Table 3 for numerical details. Insert: SEM of a gallium cut hook showing its solid composition

were separated on a 1.5% agarose gel. Later, the PCR products were submitted to Bioneer Company (Korea) and sequenced in both directions using the same PCR primers.

Sequence results were edited and trimmed using Chromas and BioEdit software. Multiple sequence alignment was performed using Clustal W method of Bioedit software. The phylogenetic tree was constructed using Maximum-Likelihood method and Tamura3-parameter model by Molecular and Evolution Genetic Analysis software version 6 (MEGA 6). Bootstrap with 1000 replications was also performed for determining the reliability of topology of the tree.

Results

Microscopical Studies

The results of microscopical comparisons of males and females of *M. cryptosaudi* n. sp., and *M. saudi* (Table 2) demonstrate that measurements of all structures are very similar in those two morphologically indistinguishable species of acanthocephalans. They were both collected from two separate but related species of hedgehogs from two

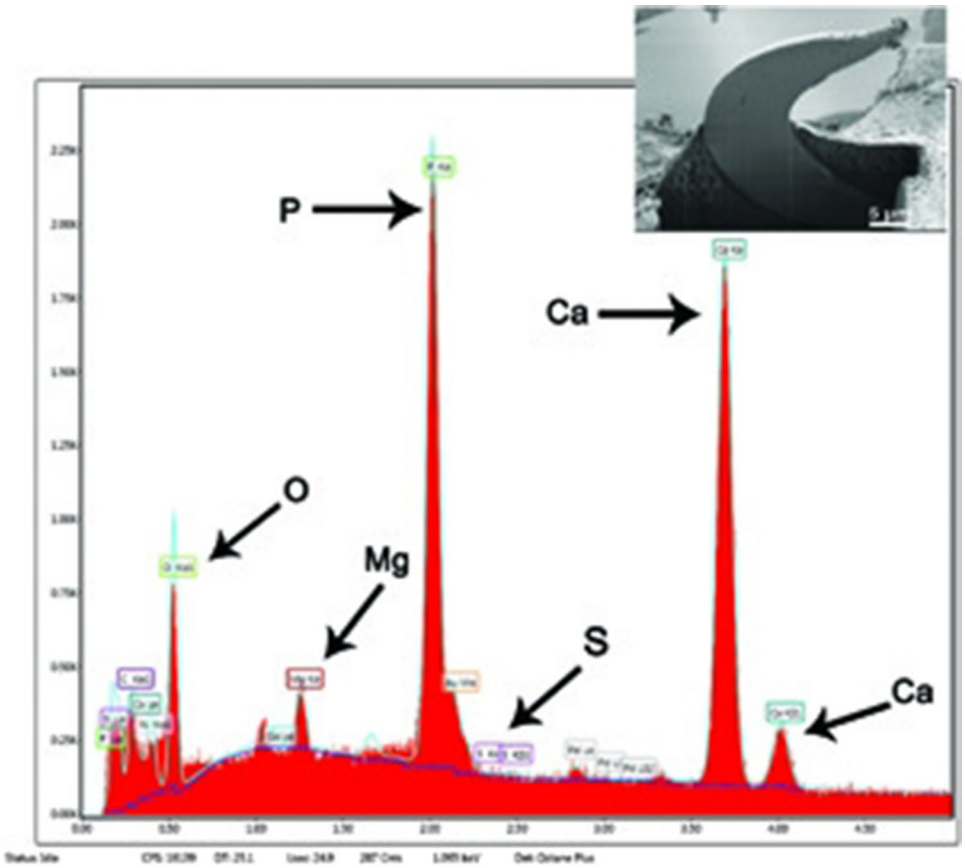

Element	Weight %	Atomic %	Error %	Net int.	K Ratio
C K	6.46	11.68	13.25	86.93	0.0183
N K	16.12	25	13.85	94.52	0.0211
O K	24.58	33.37	11.26	868.61	0.0397
Ga L	0.9	0.28	86.67	27.63	0.0056
Mg K	1.23	1.1	11.54	104.38	0.0075
P K	15.91	11.16	3.21	1405.42	0.1355
Au M	2.74	0.3	14.72	125.19	0.028
S K	0.09	0.06	61.23	7.5	0.0008
Pd L	0.83	0.17	45.73	29.99	0.0063
Ca K	31.15	16.88	2.8	1549.17	0.2797

Fig. 8 X-ray elemental scan (XEDS) of the center of a *Moniliformis kalahariensis* hook showing high levels of calcium and phosphorus comparable to those of *M. saudi* (Fig. 7); see Table 3 for numerical details. Insert: SEM of a gallium cut hook showing its solid composition

different and remote locations in east central Iraq and northeast central Saudi Arabia.

Morphological Description

The quantitative description of *M. cryptosaudi* from Iraq compared to that of *M. saudi* from Saudi Arabia is detailed in Table 2. The qualitative morphological description of *M. cryptosaudi* n. sp. is the same as that of *M. saudi* as depicted by Amin et al. [3] and the relevant figures nos. 1–24 in this paper. Additional figures nos. 1–6 of *M. cryptosaudi* show the distinct morphology of the proboscis and hooks from the Iraqi material. The porous core and surface of the collagenous proboscis hooks of *M. cryptosaudi* appear in stark contrast to the solid hooks of *M. kalahariensis* (Figs. 11, 16, 21, 32) and *M. Saudi* (Figs. 10, 12) in Amin et al. [1] and Amin et al. [3], respectively.

Taxonomic Summary

Type host: Long-eared hedgehog *Hemiechinus auritus* (Gmelin) (Erinaceidae).

Type locality: Townships around Baquba, Diyala Governerate (33°53′N 45°4′E), east-central Iraq.

Site of infection: Intestine.

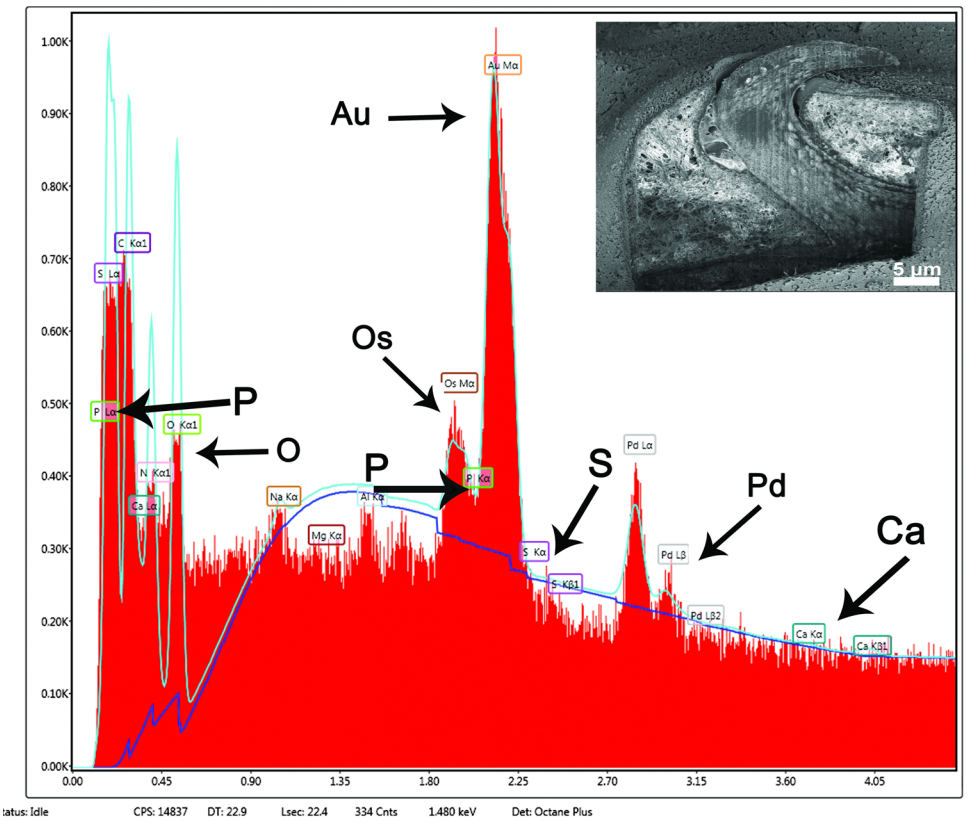

Element	Weight %	Atomic %	Error %	Net Int.	K Ratio
C K	24.09	36.79	8.1	220.29	0.1376
N K	29	37.98	13.91	101.57	0.0675
O K	18.85	21.62	13.25	112.95	0.0361
Ga L	0.64	0.17	63.23	6.76	0.0041
Mg K	0	0	99.99	0.04	0
Os M	5.24	0.51	11.76	73.47	0.0433
P K	0.44	0.26	60.17	12.71	0.0036
Au M	16.22	1.51	7.85	197.4	0.1313
S K	0.22	0.13	62.54	5.93	0.0018
Pd L	4.9	0.85	26.86	56.22	0.0351
Ca K	0.42	0.19	57.93	6.71	0.0036

Fig. 9 X-ray elemental scan (XEDS) of the center of a *Moniliformis cryptosaudi* hook showing negligible levels of calcium and phosphorus and the high content of gold and other non-hardening coating metals; see Table 3 for numerical details. Insert: SEM of a gallium cut hook showing the spongy structure of its collagenous tissue

Type material: HWML No. 139498 (holotype male and paratypes on one slide); No. 139499 (allotype female and paratypes on one slide); No. 139500 (paratypes on three slides).

Etymology: The new species name describes its cryptic status being microscopically indistinct from *M. saudi*.

Metal Analysis Using Energy Dispersive X-ray Analysis (EDXA)

The hooks of specimens of the new species appear to be of collagen material with very low levels of phosphorus and calcium at the tip, base and middle compared to those of *M. saudi* and *M. kalahariensis* having high contents of these two hardening metals (Table 3). The corresponding spectra of metals from the middle of hooks of *M. saudi*, *M. kalahariensis*, and *M. cryptosaudi* are shown in Figs. 7, 8, and 9, respectively.

Gallium Cut Hook Sections

Gallium cut hooks of *M. cryptosaudi* appeared clearly spongy, fibrous, and porous Figs. 5, 6 and inset of Fig. 9) compared to those of *M. saudi* and *M. kalahariensis*,see insets in Figs. 7 and 8.

Molecular Studies

DNA fragments of the 18S rDNA and *cox1* genes were successfully amplified and sequenced for both *M. cryptosaudi* n. sp. and *M. kalahariensis* specimens. The sequences of 18S rRNA and *cox1* genes were deposited in GenBank database (Accession Numbers: MH401040 and MH401042 for *Moniliformis kalahariensis* and also MH401041 and MH401043 for *Moniliformis cryptosaudi* n. sp.). Comparisons of the *cox1* sequences from these isolates with other available acanthocephalans sequences in GenBank, using multiple sequence alignment, revealed that the high similarity was between *M. cryptosaudi* n. sp. and *M. saudi* (99.6%), while the low similarity was between *M. cryptosaudi* n. sp. and both *M. kalahariensis* (79.0%) and *M. moniliformis* (73.7%). However, based on18S rDNA gene, *M. cryptosaudi* n. sp. had 99.4%, 99.0% and 98.9% identity with *M. saudi*, *M. kalahariensis* and *M. moniliformis*, respectively.

The phylogenetic analysis based on 18S rDNA gene revealed that *M. cryptosaudi* n. sp. and *Moniliformis saudi* are located in a sister clade to *M. kalahariensis* and *M. moniliformis* with high Bootstrap value (Fig. 10). Also, *M. cryptosaudi* n. sp. grouped as close relatives to *M. Saudi* based on the phylogenetic analysis of *cox1* gene (Fig. 11). The *cox1* amino acid sequence of *M. cryptosaudi n. sp.* had 100% similarity with *M. saudi*, but only at 89.7% and 79.4% identity with *M. kalahariensis* and *M. moniliformis*.

Discussion

The morphology and measurements of *M. cryptosaudi* and *M. saudi* suggest indistinguishable populations of acanthocephalans. Biochemical profiles and metal analysis of hooks (EDXA) are considered as diagnostic finger prints of taxonomic implications (Ha et al. [7], among others). The

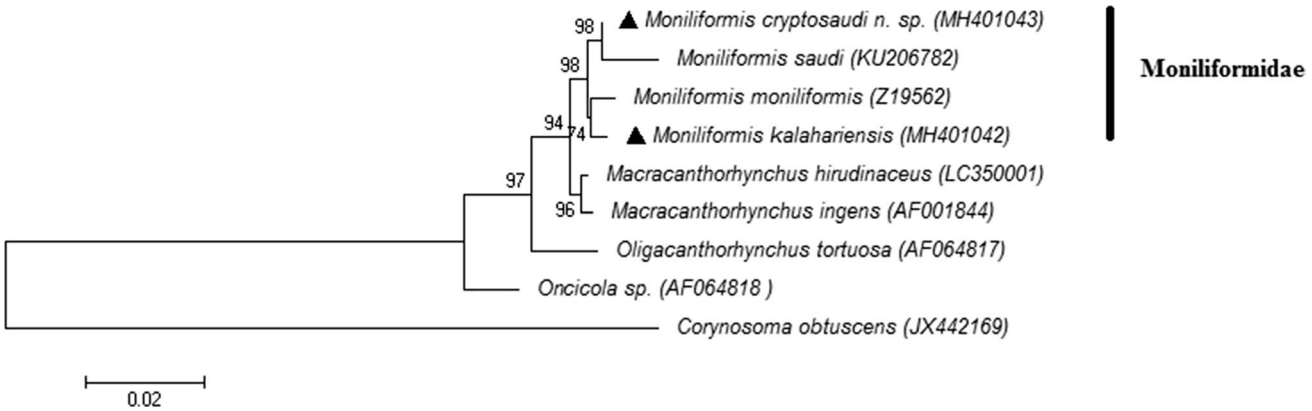

Fig. 10 Phylogenetic tree of the 18S rDNA sequences of acanthocephalans isolates obtained in this study (closed triangles) and reference sequences retrieved from GenBank. The tree was constructed by the Tamura3-parameter model in MEGA software version 6. *Corynosoma obtuscens* is used as an out group

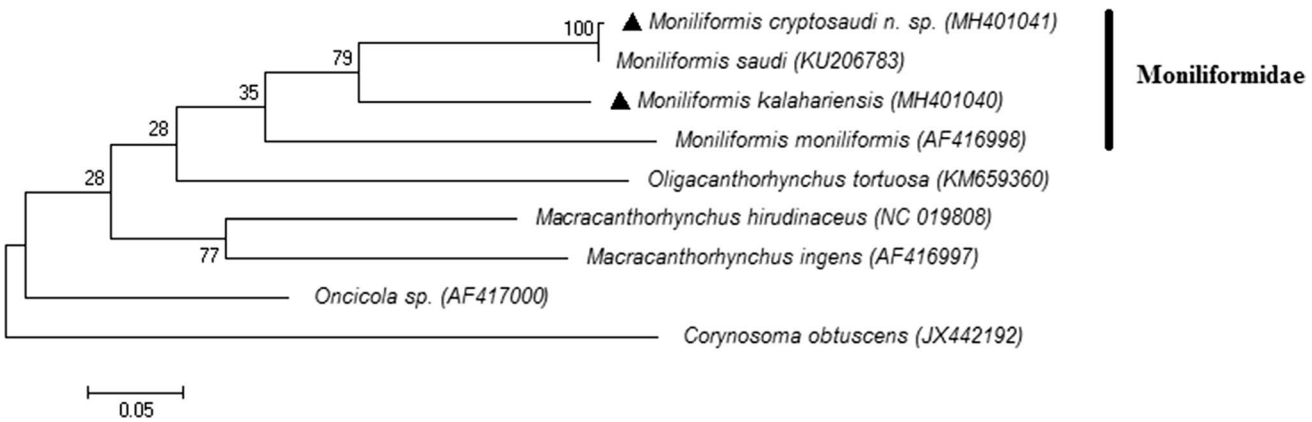

Fig. 11 Phylogenetic tree of the *cox1* sequences of acanthocephalans isolates obtained in this study (closed triangles) and reference sequences retrieved from GenBank. The tree was constructed by the Tamura3-parameter model in MEGA software version 6. *Corynosoma obtuscens* is used as an out group

different biochemical profiles and metal analysis of hooks of the two species suggest two different entities. The collagenous elements of the hooks of *M. cryptosaudi* have very low levels of the hardening metals phosphorus and calcium compared to those of *M. saudi* and *M. kalahariensis*. Collagenous tissues form structural support systems in other animals such as bones are formed by amino acids wound together in three polypeptide chains arranged in triple helices to form loose or dense reticular and elastic fibers. They are tough, fibrous proteins that have marked tensile strength and withstand forces that stretch them [8–10].

Both the 18S rDNA and *cox1* data sets revealed distinct clades of the *Moniliformis* species. Molecular finding obtained from 18S rDNA and *cox1* genes explain the morphological similarities between the *M. cryptosaudi* n. sp. and *M. saudi*. There are no differences in *cox1* amino acid sequences between *M. cryptosaudi* n. sp. and *Moniliformis saudi*. Comparisons of family Moniliformidae genes showed that the incidence of sequence differences of the *cox1* gene is higher than 18S rDNA gene. Due to the accumulation of spontaneous mutations, the rate of mitochondrial DNA evolution is about ten times faster than nuclear DNA (Brown et al. [4]. The Bootstrap values for 18S rDNA gene were higher than cox1 within acanthocephalan species. Therefore, 18S rDNA gene is the suitable marker for phylogenetic analysis of acanthocephalans. In describing *M. cryptosaudi*, we are here following the recommendations of Pérez-Ponce de León and Nadler [15] to "describe (and formally name) cryptic species following standard taxonomic practice" and are using the energy disruptive X-ray analysis (EDXA) for the first time to establish the cryptic status of this acanthocephalan.

Acknowledgements This project was supported by the Department of Biology, Brigham Young University (BYU), Provo, Utah and by an Institutional Grant from the Parasitology Center, Inc. (PCI), Scottsdale, Arizona. We thank Sarah Vorkink Child, Bean Museum (BYU) for expert help in the preparation and organization of plates.

References

1. Amin OM, Heckmann RA, Halajian A, El-NaggarA., Takavol S. (2014) Description of *Moniliformis kalahariensis* (Acanthocephala: Moniliformidae) from the South African hedgehog *Atelerix frontalis* (Erinaceidae) in South Africa. Comparative Parasitology 81:33–43
2. Amin OM, Evans RP, Boungou M, Heckmann RA (2016a) Morphological and molecular description of *Tenuisentis niloticus* (Meyer, 1932) (Acanthocephala: Tenuisentidae) from *Heterotis niloticus* (Cuvier) (Actinopterygii: Arapaimidae), in Burkina Faso, with emendation of the family diagnosis and notes on new features, cryptic genetic diversity and histopathology. Systematic Parasitology 93:173–191
3. Amin O.M., Heckmann R.A., Mohamed O., Evans R.P. 2016b. Morphological and molecular descriptions of *Moniliformis saudi* sp. n. (Acanthocephla: Moniliformidae) from the desert hedgehog *Paraechinus aethiopicus* (Ehrenberg) in Saudi Arabia, with a key to species and notes on histopathology. *Folia Parasitologica*, 63,014.
4. Brown W.M., George M. Jr., Wilson A.C. 1979. Rapid evolution of animal mitochondrial DNA. *Proceedings of the National Academy of Science, USA,* 76, 1967–1971.
5. Folmer O, Black M, Hoeh W, Lutz R, Vrijenhoek R (1994) DNA primers for amplification of mitochondrial cytochrome c oxidase subunit I from diverse metazoan invertebrates. Molecular Marine Biology and Biotechnology 3:294–299
6. Goulding TC, Cohen CS (2014) Phylogeography of a marine acanthocephalan: lack of cryptic diversity in a cosmopolitan parasite of mole crabs. Journal of Biogeography 41:965–976
7. Ha N.V., Amin O.M., Ngo H.D., Heckmann R.A. 2018. Descriptions of the acanthocephalans *Cathayacanthus spinitruncatus* (Rhadinorhynchidae) males and *Pararhadinorhynchus magnus* n. sp. (Diplosentidae) from marine fish of Vietnam, with notes on *Heterosentis holospinus* (Arhythmacanthidae). Parasite, in press
8. Hulmes D.J. 1992. The collagen superfamily—diverse structures and assemblies. *Essays in Biochemistry*, 27, 49–67. PMID 1425603.
9. Hulmes DJ (2002) Building collagen molecules, fibrils, and suprafibrillar structures. Journal of Structural Biology 137:2–10
10. Hulmes DJ, Miller A (1979) Quasi-hexagonal molecular packing in collagen fibrils. Nature 282:878–880
11. Lee RE (1992) Scanning Electron Microscopy and X-Ray Microanalysis. Prentice Hall, Englewood Cliffs, New Jersey, pp 1–464
12. Martınez-Aquino A, Reyna-Fabián ME, Rosas-Valdez R, Razo-Mendivil U, Pérez-Ponce de León G, Garcıa-Varela M (2009) Detecting a complex of cryptic species within *Neoechinorhynchus golvani* (Acanthocephala: Neoechinorhynchidae) inferred from ITSs and LSU rDNA gene sequences. Journal of Parasitology 95:1040–1047
13. Nadler SA, Pérez-Ponce de León G (2011) Integrating molecular and morphological approaches for characterizing parasite cryptic species: implications for parasitology. Parasitology 138:1688–1709
14. Near TJ, Garey JR, Nadler SA (1998) Phylogenetic relationships of the Acanthocephala inferred from 18S ribosomal DNA sequences. Molecular Phylogenetics and Evolution 10:287–98
15. Pérez-Ponce de León G, Nadler SA (2010) What we don't recognize can hurt us: a plea for awareness about cryptic species. Journal of Parasitology 96:453–464
16. Pinacho-Pinacho CD, García-Varela M, Sereno-Uribe AL, Pérez-Ponce de León G (2018) A hyper-diverse genus of acanthocephalans revealed by tree-based and non-tree-based species delimitation methods: Ten cryptic species of *Neoechinorhynchus* in Middle American freshwater fishes. Molecular Phylogenetics and Evolution 127:30–45
17. Steinauer ML, Nickol BB, Orti G (2007) Cryptic speciation and patterns of phenotypic variation of a highly variable acanthocephalan parasite. Molecular ecology 16:4097–4109
18. Zittel M, Grabner D, Wlecklik A, Sures B, Leese F, Taraschewski H, Weigand AM (2018) Cryptic species and their utilization of indigenous and non-indigenous intermediate hosts in the acanthocephalan *Polymorphus minutus sensu lato* (Polymorphidae). Parasitology 19:1–9